

Mechanical spectroscopy study of ionic liquids with quaternary cations: effect of conformational flexibility

O. Palumbo¹, A. Paolone¹, D. Rauber², C.W.M. Kay^{2,3}, F. Philippi⁴,
T. Welton⁴

¹ *Consiglio Nazionale delle Ricerche, Istituto dei Sistemi Complessi, Piazzale Aldo Moro 5,
00185 Rome, Italy*

² *Department of Chemistry, Saarland University, Campus B 2.2, 66123 Saarbrücken, Germany*

³ *London Centre for Nanotechnology, University College London, 17-19 Gordon Street, London
WC1H 0AH, UK*

⁴ *Department of Chemistry, Molecular Sciences Research Hub, Imperial College London, White
City Campus, London W12 0BZ, UK*

Abstract

Mechanical spectroscopy measurements were performed on ionic liquids (ILs) with quaternary cations, either ammonium or phosphonium, and two anions, bis(trifluoromethanesulfonyl)imide ($[\text{NTf}_2]^-$) and bis(trifluoromethanesulfonyl)methanide ($[\text{CHTf}_2]^-$), which have almost the same molecular weight and degree of fluorination but exhibit different flexibility. Furthermore, the effect of multiple ether functionalization was studied by measuring the mechanical spectrum of $[\text{P}(\text{2O2})_3\text{1}][\text{CHTf}_2]$. The measured data evidence the occurrence of a relaxation process in the liquid phase of the ILs with flexible $[\text{NTf}_2]^-$ anion and of $[\text{P}(\text{2O2})_3\text{1}][\text{CHTf}_2]$, which is analyzed by means of a modified Debye model relating the peak to the ion hopping between non-equivalent configurations. The analysis confirms the involvement of nonequivalent anion configurations as well as their energy separation. For other ILs having rigid ions, instead, a fast dynamic at local level in the liquid phase is rarely observed since a partial transition to a solid state is favored. For these liquids, the measurements suggest the formation of aggregates which is suppressed by the multiple ether functionalization.

Keywords: mechanical spectroscopy; ionic liquids; relaxation; phase transitions; conformers.

1. Introduction

Ionic liquids (ILs) present fascinating properties which make them attractive for several applications. ILs can be tailored according to the requirements of the applications, by means of a proper choice of the cation and/or the anion [1-3]. Despite the large amount of research carried out in recent years on ILs, there are still some challenges to be tackled to foster their widespread use. One of the central issues is their high viscosity, which limits liquid handling and transport properties [4,5].

Macroscopic properties are defined by microscopic properties and intermolecular interactions and, among various molecular features, a fundamental role is played by conformational flexibility [4-12]. In particular, the ions composing ILs usually present more than one conformer; in this case the ion has a high conformational flexibility when both the energy difference between the different configurations and the barrier between them is small compared to the available thermal energy [4]. Highly flexible ions are capable of fast structural reorganization on a local level, which weakens the charge network and promotes fluidity [4]. In contrast, rigid ions have, by definition, fewer degrees of freedom for relaxation. Indeed a correlation between high conformational flexibility and high ion mobility has been shown for several ions [8]. Moreover, it has been hypothesized that anion conformational relaxation correlates with translational diffusion [9-12].

Among possible choices of ions composing the ILs, those with quaternary phosphonium [4,5,8,13,14] or ammonium [13,15-17] cations are attracting considerable interest, and are still less studied than the more common imidazolium or pyrrolidinium based ILs. In particular, some phosphonium cations show promising [18, 19] properties. Generally, phosphonium based ILs have improved thermal stability compared to their ammonium analogues [20-22], and they also present lower viscosity and hence better electrical conductivity [17,23-25]. In particular, the lower viscosity is in part attributable to a more facile rotation around the P–C bond, since an increase in the barrier for the alkyl chain rotation was shown to result in a slowing down of the dynamics [8,17]. The different properties of phosphonium and ammonium ILs, which are structurally similar and only differ in the central N or P atom, have been ascribed to the flexibility of the phosphonium cations and to the more effective charge screening therein [17, 26]. Due to their interesting performance at room temperature, as well as good thermal, chemical

and electrochemical stability, phosphonium based ILs are also good candidates for batteries [4,5].

It has also been suggested that tetraalkylphosphonium cations give rise to strong ionic interactions between the oppositely charged ions which can induce the occurrence of nanoscale structural heterogeneities and strong structural correlations between oppositely charged ions [14,27]. Ether functionalization improves fluidity, ionic conductivity and diffusivity [5], in addition multiple ether functionalization has been reported to reduce the disadvantages of phosphonium ionic liquids with large cations [5]. Indeed, it is well known that ether functionalization provides an excellent mean of changing the physicochemical behavior of ionic liquids [28-31] and is particularly effective at increasing the transport properties [32] and decreasing the melting temperatures, even suppressing crystallization [28-31]. As a consequence, the exploitable temperature range for electrochemical applications widens [28-31].

Herein, we present a mechanical spectroscopy study of several ILs composed of quaternary cations and two anions having different conformational flexibility. Flexible ions are capable of a fast structural reorganization on a local level, which weakens the charge network and promotes fluidity, while rigid ions have fewer degrees of freedom for relaxation [4,5]. The experiments are performed by means of a method already successfully used for ILs [9-11] which allows the measurement of their mechanical modulus and its variation during the main phase transitions occurring at various temperatures, in both the liquid and the solid states [9-11]. The stress applied on the samples during these experiments is not a pure shear stress, thus allowing the detection of relaxations that are not necessarily observed by applying a pure shear deformation, as in the case of classic shear viscosity measurements. In particular these mechanical spectroscopy studies on ILs [9-11] showed the role of possible anion conformers on the complex relaxation dynamics of ILs, confirming that the occurrence of translational motion by means of hopping processes and molecular network rearrangements have also to be considered [12,33,34].

In particular, in the present paper we consider three different cations, methyltripentylammonium ($[N5551]^+$), methyltripentylphosphonium ($[P5551]^+$) and tris(2-ethoxyethyl)methylphosphonium ($[P(2O2)_31]^+$), which are isostructural and have similar molecular weights, and two anions, bis(trifluoromethanesulfonyl)imide ($[NTf_2]^-$) and bis(trifluoromethanesulfonyl)methanide ($[CHTf_2]^+$), which have almost the same molecular

weight and degree of fluorination but present different flexibility [4-8]. Indeed, the $[\text{CHTf}_2]^-$ anion is formally derived from the well-known $[\text{NTf}_2]^-$ by replacing the central imide group with a methanide group. Both anions have *cis*- and *trans*- conformers, but the energy barrier for the conversion between the two conformers is considerably higher for the $[\text{CHTf}_2]^-$ ion, which is therefore more rigid [4-8]. This allowed us to compare the effects of different structural modifications on the mechanical properties.

The obtained results evidence the occurrence of a relaxation process in the liquid phase of the ILs with a flexible anion and the analysis of the data provides information about the possible involvement of nonequivalent configurations as well as their energy separation. For ILs having rigid ions, instead, a fast dynamic at local level in the liquid phase is rarely observed since a partial transition to a solid state is favored. For these liquids, the measurements seem also to suggest the formation of aggregates, whose organization can result in domain formation.

2. Materials and Methods

Ionic liquids composed of quaternary cations: $[\text{N5551}]^+$, $[\text{P5551}]^+$, $[\text{P(2O2)}_3\text{1}]^+$, and fluorinated anions: $[\text{NTf}_2]^-$ and $[\text{CHTf}_2]^-$, namely $[\text{N5551}][\text{NTf}_2]$, $[\text{P5551}][\text{NTf}_2]$, $[\text{N5551}][\text{CHTf}_2]$, $[\text{P5551}][\text{CHTf}_2]$, and $[\text{P(2O2)}_3\text{1}][\text{CHTf}_2]$ (Figure 1) were synthesized as described in the literature [4].

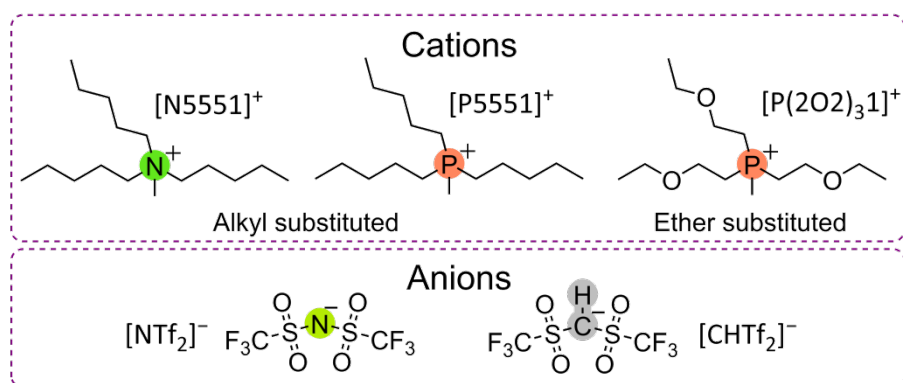


Figure 1. Structure of ions composing the ILs studied in the present work.

Dynamic mechanical analysis (DMA) was carried out using a PerkinElmer DMA 8000 instrument, by means of a method already used in previous works [9-11]: at room temperature the liquid samples were laid out into a stainless steel Material Pocket, supplied by PerkinElmer (30.0 mm by 14.0 mm by 0.5 mm), which is scored in the mid-point. The pocket was then folded

in half and crimped closed. Flexural vibration measurements were performed in the three-point bending configuration. The storage modulus, M , and the elastic energy dissipation, $\tan \delta$, were measured in an inert nitrogen atmosphere, at variable frequencies (1 and 10 Hz in the present case) and scanning temperature at 4 K min^{-1} in the range between 160 and 350 K. With this setup, the stress applied on the sample is not a pure shear stress, but, due to the spatial isotropy of liquids, the mechanical modulus presently measured is a combination of both the shear and the bulk modulus [35,36].

When species can move between two configurations with a relaxation rate τ^{-1} by means of thermal activation in a standard anelastic solid [37], the elastic energy dissipation presents a maximum when the Debye relaxation condition, $\omega\tau = 1$, is satisfied. For a single relaxation time, τ , $\tan \delta$ is given by:

$$\tan \delta = \Delta(T) \frac{1}{(\omega\tau)^{-\alpha} + (\omega\tau)^{\alpha}} \quad (1)$$

where ω is the angular vibration frequency and the relaxation intensity, (Δ) , is proportional to the concentration of the relaxing species, to the elastic modulus and to the change in the local distortion, α is the Fuoss–Kirkwood width parameter and is equal to 1 for a single time Debye relaxation; $\alpha < 1$ produces broadened peaks with respect to Debye ones.

One can assume for the relaxation time τ a Vogel-Fulcher-Tammann type (VFT) temperature dependence:

$$\tau = \tau_0 e^{\left[\frac{W}{k(T-T_0)} \right]} \quad (2)$$

where W is the activation energy and T_0 is the temperature parameter. Indeed, the empirical VFT formula has been largely used to describe the temperature dependence of several physical properties of ionic liquids above the glass transition, such as the conductivity and the inverse of the viscosity [4,5], as observed in many other glass forming liquids.

If the relaxation occurs between two equivalent sites, the relaxation intensity in Eq. (1) decreases with increasing T , leading to a higher intensity for the peaks measured at lower frequencies. Instead, in the case of hopping between two nonequivalent configurations with energy separation ΔE , the relaxation intensity, which is proportional to the product of the respective populations in the two configurations, becomes [9-11]:

$$\Delta(T) \propto \frac{c}{T} \operatorname{sech}^2\left(\frac{\Delta E}{2kT}\right) \quad (3)$$

Considering equations 1 and 3, a more general expression for $\tan \delta$ is then given by:

$$\tan \delta = \frac{c}{T \cosh^2(\Delta E/2kT)} \frac{1}{(\omega\tau)^{-\alpha} + (\omega\tau)^\alpha} \quad (4)$$

3. Results and Discussion

Figure 2 displays the DMA spectra (modulus, M , and $\tan \delta$) of samples sharing the $[\text{NTf}_2]^-$ anion measured on cooling at 4 K min^{-1} . The storage modulus is reported as the variation with respect to the value measured around room temperature because it is not possible to separate the contribution of the ILs from that of the pocket, which, as already shown elsewhere [9-11], has to be considered as a background.

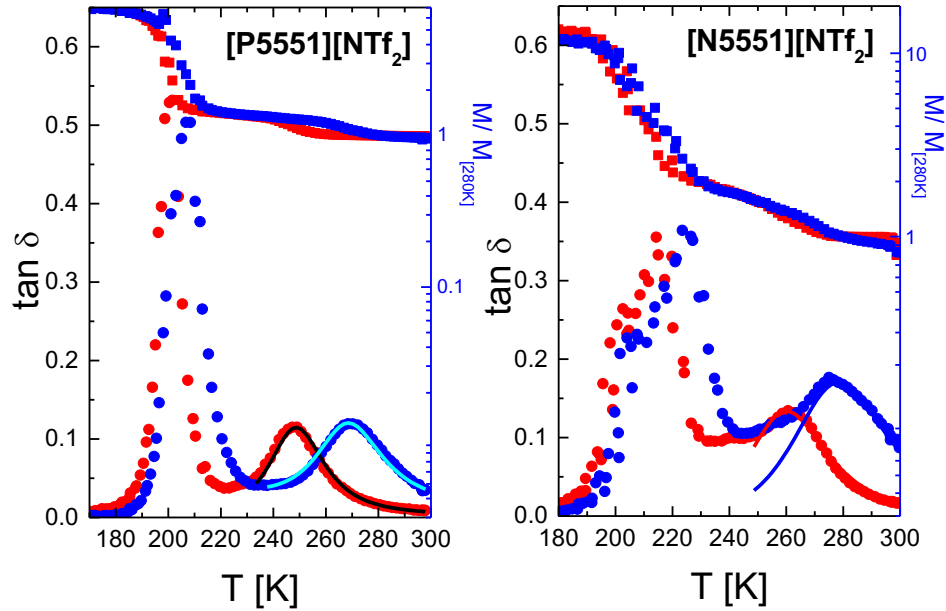


Figure 2. DMA spectra of the samples $[\text{P5551}][\text{NTf}_2]$ and $[\text{N5551}][\text{NTf}_2]$, measured inside the pocket on cooling at two frequencies (blue 10Hz, red 1Hz). The continuous thick line is a fit according to Eqs 1–4 for the thermally activated peak.

The spectrum of the $[\text{P5551}][\text{NTf}_2]$ displays the occurrence of a thermally activated relaxation process around 250 K (for a vibration frequency of 1 Hz). Indeed, at this temperature the $\tan \delta$

curve shows a peak, whose maximum shifts to higher temperature with increasing frequency (~ 270 K for a vibration frequency of 10 Hz; see Fig. 2), and concomitantly, a step is observed in the modulus (Fig. 2). On further cooling, around 190 K, the anelastic spectra shows an intense stiffening of the modulus and an intense peak of $\tan\delta$. These last features indicate the occurrence of the glass transition, in agreement with previous DSC data [4,5]. Similar features are observed also in the spectrum of sample [N5551][NTf₂] (Fig. 2). On cooling a thermally activated peak appears around 260 K (for a vibration frequency of 1 Hz), accompanied by a concomitant step in the modulus and, on further cooling, around 200 K the typical features of the glass transition, i.e. intense stiffening of the modulus and an intense peak of $\tan \delta$, are displayed. The temperature measured for the glass transition is in agreement with previously reported calorimetric measurements [4,5]. However, the thermally activated process displayed by [N5551][NTf₂] seems to be slightly broader compared to the one measured for the phosphonium containing IL and, indeed, the peak shown by $\tan \delta$ is not fully resolved since its low temperature side is partially superimposed on another peak appearing at lower temperature and attributed to the glass transition. However, for both samples it was possible to reasonably fit the data of the two frequencies (continuous lines in Fig. 2) using Eq. 4, which is appropriate for jumps in an asymmetrical potential well, and assuming for the relaxation time (τ) a Vogel–Fulcher–Tamman type (VFT) temperature dependence (Eq. 2). This model has been already successfully used to fit similar relaxation processes found in the supercooled liquid phase of ILs having the same ([NTf₂]⁻) or other perfluorinated anions [9-11] of those ones presently reported. The values of the best-fit parameters are reported in Table 1.

	τ_0 [s]	T_0 [K]	α	E [eV]	ΔE [meV]
[P5551][NTf ₂]	$(4.1 \pm 0.1)10^{-13}$	35 ± 5	0.9 ± 0.1	0.49 ± 0.02	27 ± 3
[N5551][NTf ₂]	$(1.5 \pm 0.2)10^{-13}$	56 ± 5	0.6 ± 0.2	0.49 ± 0.02	27 ± 7
[P(2O2) ₃ 1][CHTf ₂]	$(1.0 \pm 0.1)10^{-13}$	88 ± 8	0.95 ± 0.02	0.32 ± 0.01	52 ± 8

Table1. Best fit parameters obtained for the relaxation processes in the three ILs.

The values obtained for the pre-exponential factor of the relaxation time and the activation energy are in good agreement with previous literature [9-11], while the width parameter α lower than 1 indicates interaction among the relaxing units. The value for the energy separation of the

nonequivalent configurations (ΔE) is the same for the two samples, i.e. 27 ± 3 meV, and it is close to the energy separations measured for other ILs having the same $[\text{NTf}_2]^-$ anion and well comparable to the energy separations obtained by calculations for the *trans* and *cis* $[\text{NTf}_2]^-$ anion conformers [4,5,9,38-40].

The DMA spectra (modulus, M , and $\tan \delta$) measured on cooling for the samples having the $[\text{CHTf}_2]^-$ anion are reported in Figure 3.

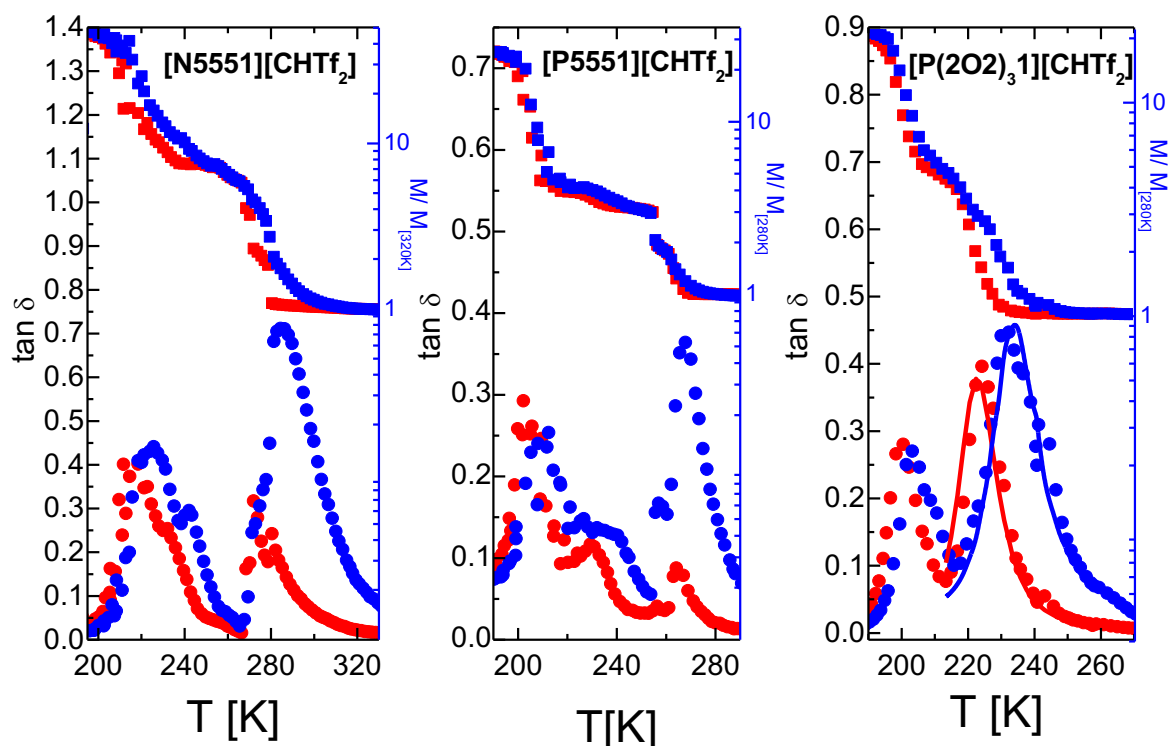


Figure 3. DMA spectra of the samples $[\text{N5551}][\text{CHTf}_2]$, $[\text{P5551}][\text{CHTf}_2]$ and $[\text{P}(\text{2O}_2)_3]_1[\text{CHTf}_2]$ measured inside the pocket on cooling at 4 Kmin^{-1} and at two frequencies (blue 10Hz, red 1Hz). The continuous thick line is a fit according to Eqs. 1–4 for the thermally activated peak of $[\text{P}(\text{2O}_2)_3]_1[\text{CHTf}_2]$.

The spectra of $[\text{P5551}][\text{CHTf}_2]$ and $[\text{N5551}][\text{CHTf}_2]$ are similar. On cooling, they both display a first pronounced peak in the $\tan \delta$ accompanied by an intense step in the modulus curve, at 280 and 265 K for the $[\text{N5551}][\text{CHTf}_2]$ and the $[\text{P5551}][\text{CHTf}_2]$ sample, respectively. These features are not thermally activated since their maximum does not shift at higher temperature

with increasing frequency and are more likely attributable to the occurrence of a phase transition. The larger variation of the modulus value, compared to the one observed for the relaxation process in the $[\text{NTf}_2]^-$ analogues previously discussed, further confirms this attribution. Indeed, for thermally activated relaxation in Fig. 2 the modulus almost doubles its value, while the variations observed around 280 and 265 K for the $[\text{CHTf}_2]^-$ samples induce an increase of six or eight times in the normalized modulus. Also, the peak in $\tan\delta$ is very intense with values at the maximum similar to those previously observed for glass transitions in the $[\text{NTf}_2]^-$ samples. For the $[\text{N5551}][\text{CHTf}_2]$ a crystallization temperature of 281 K has been reported [4,5] thus suggesting that the observed transition could be related to the occurrence of solidification.

However, on further cooling an additional transition is observed around 200 K for the $[\text{P5551}]^+$ sample (220 K for the $[\text{N5551}]^+$ sample), which is similar to a glass transition. Indeed, for $[\text{P5551}][\text{CHTf}_2]$ the occurrence of a glass transition has been reported at 200 K [4,5]. The observation of both transitions (possible solidification and transition to a glassy state) suggests a non-homogeneity in the sample, which likely only partially crystallizes on cooling, while the remaining part displays undercooling. It must be pointed out that the samples were all measured on cooling after heating to 80°C in order to make them as homogeneous as possible and to erase their thermal history.

Measurements carried out on heating back to room temperature and reported in the supporting info (Figure S1) show that both $[\text{N5551}][\text{CHTf}_2]$ and $[\text{P5551}][\text{CHTf}_2]$ display a glass transition and a cold crystallization on further heating (whose signature is an increase in the modulus around 230 (220) K for $[\text{N5551}][\text{CHTf}_2]$ ($[\text{P5551}][\text{CHTf}_2]$)) and finally a subsequent melting around 290 (280) K, in agreement with previously reported data [4,5]. A similar behavior has been reported for other ILs [9-11] and confirms that at least part of the samples is undercooled into a glassy state.

The occurrence of partial solidification on cooling in these samples could be related to occurrence of aggregation and clustering in quaternary cations [4,5]. In particular for $[\text{NTf}_2]^-$ containing ILs with phosphonium cations this tendency is reduced, while it is more evident in ILs with non-fluorinated anions. The occurrence of a higher level of clustering would result in an increased inhomogeneity of samples and thus in the observation of partial crystallization of the $[\text{CHTf}_2]^-$ samples, despite the same thermal treatment of their $[\text{NTf}_2]^-$ analogues.

Partial solidification, *i.e.* the coexistence of solid and liquid phases, has been reported previously [41-43]. However, the size of the liquid pockets is not known, this would be an interesting subject for future studies. The spectrum of the ether functionalized $[P(2O2)_3]_1[CHTf_2]^-$ sample (Fig. 3) on cooling presents a peak accompanied by a stiffening of the modulus around 220 K (for a vibration frequency of 1 Hz) which is thermally activated since the maximum shifts to higher temperatures with increasing vibration frequency. It is worth noting that the intensity of the relaxation peak and of the concomitant modulus variation are larger than those observed for the relaxation processes in the $[NTf_2]^-$ samples and are even more intense than those displayed by the non-thermally activated process observable in the $[P(2O2)_3]_1[CHTf_2]^-$ spectrum on further cooling. The latter process, well visible as a peak in the $\tan\delta$ accompanied by an increase of the modulus, is likely due to the occurrence of the glass transition around 200 K. This value for the glass transition temperature is indeed in agreement with the previously literature data of 197 K [4]. Measurements carried out on heating back to room temperature and reported in the supporting info (Figure S2) show that the same features are displayed also on heating back. Therefore, the behavior of the sample on heating is quite similar to that observed on cooling, as on increasing temperature it undergoes a transition from the glass to the liquid phase and in this latter phase it displays the same relaxation reported on cooling.

The relaxation process displayed by the $[P(2O2)_3]_1[CHTf_2]^-$ sample on cooling was fitted by the same model previously used for the $[NTf_2]^-$ samples. The best fit curves are displayed in Fig. 3 and the best fit parameters are reported in Table 1.

The values obtained for the pre-exponential factor of the relaxation time and the width parameter are in good agreement with those displayed by the $[NTf_2]^-$ samples. The activation energy, 0.32 ± 0.01 eV, is lower than those obtained for the other two samples. This lower value for the energy barrier of the relaxation would be in agreement with the accelerated dynamics already observed in terms of increased diffusivity and ionic conductivity for quaternary ILs with ether containing side chains [4]. It is worth noting that the activation energy is related to the whole relaxing unit, which likely conveys also the presence of the multiple ether functionalized cation. Conversely, the value for the energy separation of the nonequivalent *trans* and *cis* configurations of the $[CHTf_2]^-$ anion, *i.e.* 52 ± 8 meV, is almost twice the energy separations obtained for the ILs having the $[NTf_2]^-$ anion. This is in agreement with the calculated higher energy separation between the two lowest energy conformers of the $[CHTf_2]^-$ anion compared to its more flexible

isoelectronic [NTf₂]⁻ analogue [4,5]. This result further confirms the role of the anion conformer flexibility on the dynamic processes occurring in ILs. Moreover, similar to the models usually used to describe relaxation peaks by mechanical spectroscopy in solids, it would be possible to hypothesize that an increased intensity in the relaxation process (the intensity of the peak observed in the [P(2O2)₃1][CHTf₂] is almost the double of those displayed by [N5551][CHTf₂] and [P5551][CHTf₂]) could be related to an increase of the local deformation involved in the relaxation, just like the elastic dipole in solids. This could be explained in terms of an increased local ionic rearrangement during the relaxation, likely connected to the increased rigidity of the [CHTf₂]⁻ anion whose relaxation mechanism is less assisted by conformational flexibility and thus involve rigid local movements of the same conformer.

Moreover, for the [P(2O2)₃1] the side chains curl up [5] and possibly decrease the interaction between cation and anion, thus facilitating the sliding motion of the two ions. This sliding motion indeed results in the DMA spectrum in a relaxation with a lower activation energy and a bigger local distortion as the two ions are more isolated by the chains curling [44-49].

It is worth noting that the [P(2O2)₃1][CHTf₂] sample does not display any partial solidification, conversely to the observations for the other two [CHTf₂]⁻ containing ILs. In this framework the higher homogeneity displayed by the former sample is likely due to the ether functionalization, which has been found to prevent or at least suppresses segregation in ILs with alkylphosphonium or alkylammonium cations [4], and further confirms that the partial crystallization reported for [N5551][CHTf₂] and [P5551][CHTf₂] can be related to occurrence of clustering. Moreover, this behavior is also in agreement with the largely reported suppression of crystallization in ether-functionalized ILs [28-31].

4. Conclusions

The mechanical spectra of ILs with quaternary cations having similar structures differing only in the central atom of the cation, ammonium or phosphonium, and anions with different flexibility were measured, together with one sample with an ether substituted phosphonium cation. The relaxation processes measured in the ILs liquid phase allowed the study of the ions dynamics which has been described by the ion hopping between non-equivalent configurations. These configurations are strongly affected by the different anion conformers, further confirming the central role of the ion flexibility in the dynamical processes in ILs. Moreover, for ILs having

rigid ions, a partial transition to a solid state is reported and it is attributed to the formation of aggregates, which seems to be suppressed by multiple ether functionalization.

Acknowledgements

This work has received funding from the Joint Bilateral Agreement CNR/Royal Society (UK) - Biennial Programme 2022-2023 - prot. number 0082091-2021.

REFERENCES

- [1] T. Welton, Ionic liquids: a brief history, *Biophys. Rev.* 10 (2018) 691–706.
- [2] M. Armand, F. Endres, D. R. MacFarlane, H. Ohno and B. Scrosati, Ionic-liquid materials for the electrochemical challenges of the future, in *Materials for Sustainable Energy*, World Scientific, 2011, 129–137.
- [3] O. Palumbo, F. Trequattrini, M.A. Navarra, J.-B. Brubach, P. Roy, A. Paolone, Tailoring the physical properties of the mixtures of ionic liquids: a microscopic point of view, *Phys. Chem. Chem. Phys.* 19 (2017) 8322–8329.
- [4] F. Philippi, D. Rauber, B. Kuttich, T. Kraus, C.W.M. Kay, R. Hempelmann, P.A. Hunt and T. Welton, Ether functionalization, ion conformation and the optimisation of macroscopic properties in ionic liquids, *Phys. Chem. Chem. Phys.* 22 (2020) 23038–23056.
- [5] F. Philippi, D. Rauber, J. Zapp, C. Präsang, D. Scheschkewitz and R. Hempelmann, Multiple Ether-Functionalized Phosphonium Ionic Liquids as Highly Fluid Electrolytes *Chem. Phys. Chem.* 20 (2019) 443–455.
- [6] F. Philippi, D. Rauber, J. Zapp and R. Hempelmann, Transport properties and ionicity of phosphonium ionic liquids, *Phys. Chem. Chem. Phys.* 19(2017) 23015–23023.
- [7] F. Philippi and T. Welton, Targeted modifications in ionic liquids – from understanding to design, *Phys. Chem. Chem. Phys.* 23 (2021) 6993–7021.
- [8] F. Philippi, D. Pugh, D. Rauber, T. Welton and P. A. Hunt, Conformational design concepts for anions in ionic liquids, *Chem. Sci.* 11(2020) 6405–6422.
- [9] O. Palumbo, F. Trequattrini, F. M. Vitucci, A. Paolone, Relaxation dynamics and phase transitions in ionic liquids: viscoelastic properties from the liquid to the solid state, *J. Phys. Chem. B* 119 (2015) 12905–12911.

- [10] A. Paolone, O. Palumbo, F. Trequattrini, G. B. Appetecchi, Relaxational dynamics in the PYR14-IM14 ionic liquid by mechanical spectroscopy. *Mat. Res.* 21 suppl2 (2018) e20170870.
- [11] F. Trequattrini, A. Paolone, O. Palumbo, F.M. Vitucci, M. A. Navarra, S. Panero, Low Frequency Mechanical Spectroscopy Study of Three Pyrrolidinium Based Ionic Liquids, *Arch. Met. Mat.* 60 (2015) 385–390.
- [12] S. N. Suarez, A. Rúa, D. Cuffari, K. Pilar, J. L. Hatcher, S. Ramati and J. F. Wishart, Do TFSA anions slither? Pressure exposes the role of TFSA conformational exchange in self-diffusion, *J. Phys. Chem. B* 119(2015) 14756–14765.
- [13] O. Palumbo A. Sarra, J.-B. Brubach, F. Trequattrini, A. Cimini, S. Brutti, G. B. Appetecchi, E. Simonetti, G. Maresca, S. Fantini, R. Lin, A. Falgayrat, P. Roy, A. Paolone, So Similar, yet so Different: The Case of the Ionic Liquids N-Trimethyl-N (2-methoxyethyl)ammonium Bis (trifluoromethanesulfonyl)imide and N,N-Diethyl-N-methyl-N(2-methoxyethyl)ammonium bis(trifluoromethanesulfonyl)imide, *Frontiers in Physics* 10 (2022) 851279.
- [14] L. Gontrani, O. Russina, F. Lo Celso, R. Caminiti, G. Annat, and A. Triolo, Liquid structure of trihexyltetradecylphosphonium chloride at ambient temperature: an X-ray scattering and simulation study, *J. Phys. Chem. B* 113 (2009) 9235–9240.
- [15] J. Sun, M. Forsyth and D. R. MacFarlane, Room-temperature molten salts based on the quaternary ammonium ion, *J. Phys. Chem. B* 102 (1998) 8858–8864.
- [16] D. R. MacFarlane, J. Sun, J. Golding, P. Meakin and M. Forsyth, High conductivity molten salts based on the imide ion, *Electrochim. Acta* 45 (2000) 1271–1278.
- [17] L. K. Scarbath-Evers, P. A. Hunt, B. Kirchner, D. R. MacFarlane and S. Zahn, Molecular features contributing to the lower viscosity of phosphonium ionic liquids compared to their ammonium analogues, *Phys. Chem. Chem. Phys.* 17 (2015) 20205–20216.
- [18] K. J. Fraser, D. R. MacFarlane, Phosphonium-based ionic liquids: an overview, *Aust. J. Chem.* 62, (2009) 309–321.

- [19] M. D. Green, C. Schreiner, T. E. Long, Thermal, rheological, and ion-transport properties of phosphonium-based ionic liquids, *J. Phys. Chem. A* 115 (2011) 13829–13835.
- [20] B. Wang, L. Qin, T. Mu, Z. Xue, G. Gao, Are ionic liquids chemically stable? *Chem. Rev.* 117 (2017) 7113–7131.
- [21] N. De Vos, C. Maton, C. V. Stevens, Electrochemical stability of ionic liquids: general influences and degradation mechanisms, *ChemElectroChem* 1 (2014) 1258–1270.
- [22] K. Tsunashima, E. Niwa, S. Kodama, M. Sugiya and Y. Ono, Thermal and transport properties of ionic liquids based on benzyl-substituted phosphonium cations, *J. Phys. Chem. B* 113 (2009) 15870–15874.
- [23] U. A. Rana, R. Vijayaraghavan, M. Walther, J. Sun, A. A. J. Torriero, M. Forsyth and D. R. MacFarlane, Protic ionic liquids based on phosphonium cations: comparison with ammonium analogues, *Chem. Commun.* 47(2011) 11612–11614.
- [24] J. A. Vega, J. Zhou and P. A. Kohl, Electrochemical comparison and deposition of lithium and potassium from phosphonium and ammonium-TFSI ionic liquids, *J. Electrochem. Soc.* 156 (2009) A253–A259.
- [25] S. Seki, K. Hayamizu, S. Tsuzuki, K. Fujii, Y. Umebayashi, T. Mitsugi, T. Kobayashi, Y. Ohno, Y. Kobayashi, Y. Mita, H. Miyashiro and S. Ishiguro, Relationships between center atom species (N, P) and ionic conductivity, viscosity, density, self-diffusion coefficient of quaternary cation room-temperature ionic liquids, *Phys. Chem. Chem. Phys.* 11 (2009) 3509–3514.
- [26] M. H. Ghatee and M. Bahrami, Emergence of innovative properties by replacement of nitrogen atom with phosphorus atom in quaternary ammonium ionic liquids: Insights from ab initio calculations and MD simulations, *Chem. Phys.* 490 (2017) 92–105.
- [27] K. J. Fraser, E. I. Izgorodina, M. Forsyth, J. L. Scott, D. R. MacFarlane, Liquids intermediate between “molecular” and “ionic” liquids: Liquid Ion Pairs? *Chem. Commun.* 37 (2007) 3817–3819.

- [28] O. Palumbo, F. Trequattrini, A. Tsurumaki, M. A. Navarra and A. Paolone, The effect of ether-functionalisation on the inter and intra-molecular interactions in ionic liquids. *J. Phys. Chem. B* 125 (2021) 2380–2388.
- [29] A. Tsurumaki, F. Trequattrini, O. Palumbo, S. Panero, A. Paolone, M. A. Navarra, The effect of ether-functionalisation in ionic liquids analysed by DFT calculation, infrared spectra, and Kamlet-Taft parameters, *Phys. Chem. Chem. Phys.* 20 (2018) 7989–7997.
- [30] M. A. Navarra, K. Fujimura, M. Sgambetterra, A. Tsurumaki, S. Panero, N. Nakamura N, H. Ohno, B. Scrosati, New ether-functionalized morpholinium and piperidinium-based ionic liquids as electrolyte components in lithium and lithium-ion batteries. *ChemSusChem* 10 (2017) 2496–2504.
- [31] A. Tsurumaki, H. Ohno, S. Panero, M. A. Navarra. Novel bis(fluorosulfonyl) imide-based and ether-functionalized ionic liquids for lithium batteries with improved cycling properties. *Electrochim. Acta* 293 (2019) 160–165.
- [32] K. R. Harris, T. Makino and M. Kanakubo, Viscosity scaling of the self-diffusion and velocity cross-correlation coefficients of two functionalised ionic liquids and of their non-functionalized analogues, *Phys. Chem. Chem. Phys.* 16 (2014) 9161–9170.
- [33] F. Castiglione, M. Moreno, G. Raos, A. Famulari, A. Mele, G. B. Appetecchi, S. Passerini, Structural organization and transport properties of novel pyrrolidinium-based ionic liquids with perfluoroalkyl sulfonylimide anions. *J. Phys. Chem. B* 113 (2009) 10750–10759.
- [34] S. Schrödle, G. Annat, D. R. MacFarlane, M. Forsyth, R. Buchner, G. Hefter, High frequency dielectric response of the ionic liquid N-methyl-N-ethylpyrrolidinium dicyanamide. *Aust. J. Chem.* 50 (2007) 6–8.
- [35] T. Yamaguchi, S. Miyake, and S. Koda, Shear relaxation of imidazolium-based room-temperature ionic liquids, *J. Phys. Chem. B* 114 (2010) 8126–8133.
- [36] W. Makino, R. Kishikawa, M. Mizoshiri, S. Takeda, and M. Yao, Viscoelastic properties of room temperature ionic liquids, *J. Chem. Phys.* 129 (2008) 104510–104517.

- [37] A. S. Nowick, B. S. Berry, *Anelastic Relaxation in Crystalline Solids*; Academic Press: New York, 1972.
- [38] M. Herstedt, M. Smirnov, P. Johansson, M. Chami, J. Grondin, L. Servant, J. C. Lassegues, Spectroscopic Characterization of the Conformational States of the Bis(trifluoromethanesulfonyl)imide Anion (TFSI⁻). *J. Raman Spectrosc.* 36 (2005) 762–770.
- [39] F. M. Vitucci, F. Trequattrini, O. Palumbo, J.-B. Brubach, P. Roy, A. Paolone, Infrared spectra of bis(trifluoromethanesulfonyl)-imide based ionic liquids: experiments and ab-initio simulations. *Vib. Spectrosc.* 74 (2014) 81–87.
- [40] O. Palumbo, F. Trequattrini, F. M. Vitucci, M. A. Navarra, S. Panero, A. Paolone An infrared spectroscopy study of the conformational evolution of the bis(trifluoromethanesulfonyl)imide ion in the liquid and in the glass state. *Adv. Cond. Mat.* 2015 (2015) 176067.
- [41] M. Y. Ivanov, S. A. Prikhod'ko, N. Y. Adonin, I. A. Kirilyuk, S. V. Adichtchev, N. V. Surovtsev, S. A. Dzuba, and M. V. Fedin, Structural anomalies in ionic liquids near the glass transition revealed by pulse EPR, *J. Phys. Chem. Lett.* 9 (2018) 4607–4612.
- [42] A. E. Khudozhitkov, P. Stange, A. G. Stepanov, D. I. Kolokolov and R. Ludwig, Structure, hydrogen bond dynamics and phase transition in a model ionic liquid electrolyte, *Phys. Chem. Chem. Phys.* 24 (2022) 6064–6071.
- [43] A. E. Khudozhitkov, P. Stange, B. Golub, D. Paschek, A. G. Stepanov, D. I. Kolokolov, R. Ludwig, Characterization of doubly ionic hydrogen bonds in protic ionic liquids by NMR deuteron quadrupole coupling constants: differences to H-bonds in amides, peptides, and proteins, *Ang. Chemie Int. Ed.* 56 (2017) 14310–14314.
- [44] J. C. Araque, J. J. Hettige, and C. J. Margulis, Modern room temperature ionic liquids, a simple guide to understanding their structure and how it may relate to dynamics, *J. Phys. Chem. B* 119 (2015) 12727–12740.

- [45] H. K. Kashyap, C. S. Santos, R. P. Daly, J. J. Hettige, N. S. Murthy, H. Shirota, E. W. Castner, Jr. and C. J. Margulis, How does the ionic liquid organizational landscape change when nonpolar cationic alkyl groups are replaced by polar isoelectronic diethers?, *J. Phys. Chem. B* 117 (2013) 1130–1135.
- [46] D. Rauber, F. Philippi, B. Kuttich, J. Becker, T. Kraus, P. Hunt, T. Welton, R. Hempelmann and C. W. M. Kay, Curled cation structures accelerate the dynamics of ionic liquids, *Phys. Chem. Chem. Phys.* 23 (2021) 21042–21064.
- [47] K. Yoshii, T. Uto, N. Tachikawa and Y. Katayama, The effects of the position of the ether oxygen atom in pyrrolidinium-based room temperature ionic liquids on their physicochemical properties, *Phys. Chem. Chem. Phys.* 22 (2020) 19480–19491.
- [48] K. Shimizu, C. E. S. Bernardes, A. Triolo and J. N. Canongia Lopes, Nano-segregation in ionic liquids: scorpions and vanishing chains, *Phys. Chem. Chem. Phys.* 15 (2013) 16256–16262.
- [49] H. J. Zeng, M. A. Johnson, J. D. Ramdihal, R. A. Sumner, C. Rodriguez, S. I. Lall-Ramnarine, and J. F. Wishart, Spectroscopic assessment of intra- and intermolecular hydrogen bonding in ether-functionalized imidazolium ionic liquids, *J. Phys. Chem. A* 123 (2019) 8370–8376.

Supporting Info

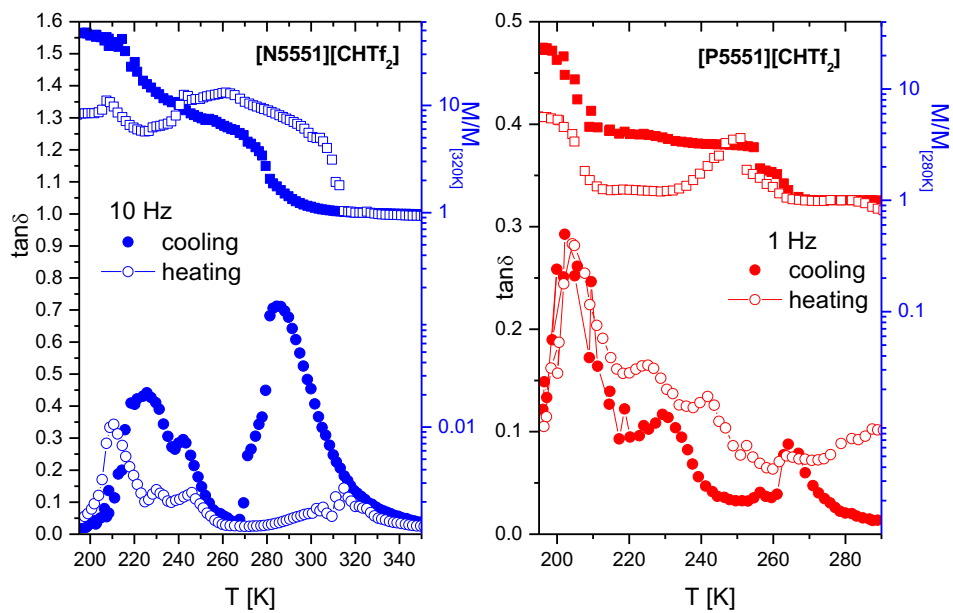


Figure S1. DMA spectra of the samples [N5551][CHTf₂], [P5551][CHTf₂] measured inside the pocket on cooling and heating at 4 Kmin⁻¹.

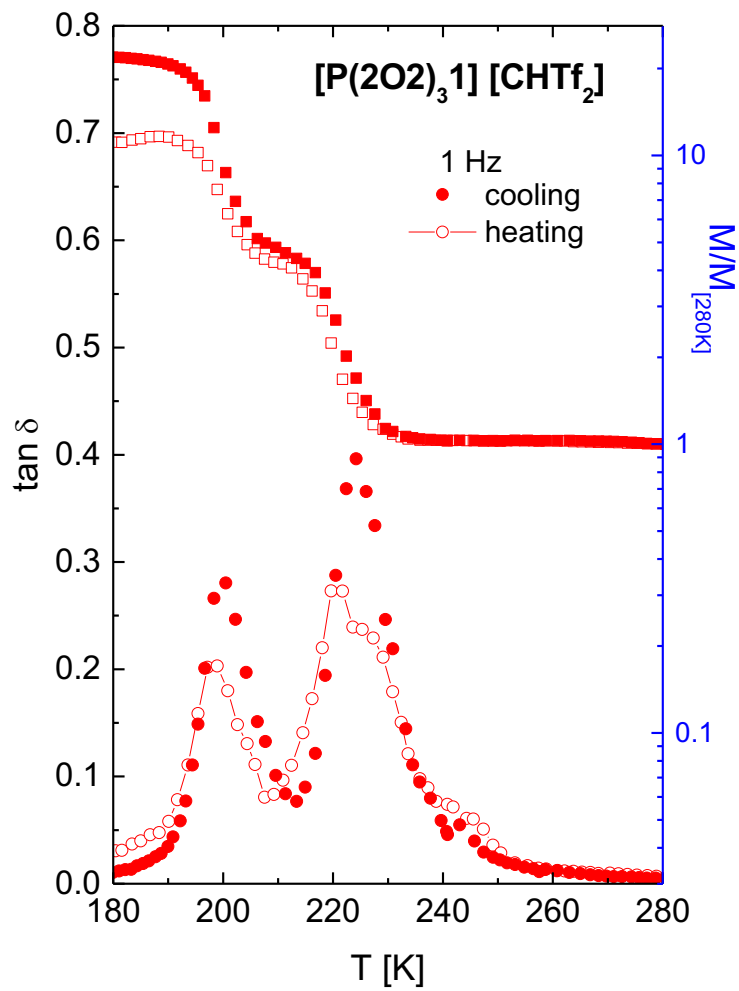


Figure S2. DMA spectra of the sample $[P(2O_2)_3]_1[CHTf_2]$ measured inside the pocket on cooling and heating at 4 Kmin^{-1} .